Stereochemical studies on nucleic acid analogues. I. Conformations of ?-nucleosides and ?-nucleotides: Interconversion of sugar puckers via O4?-exo

ARTICLE *in* BIOPOLYMERS · MARCH 1992

Impact Factor: 2.39 · DOI: 10.1002/bip.360320306 · Source: PubMed

2 AUTHORS:

Swarnalatha Y. Reddy

22 PUBLICATIONS **235** CITATIONS

SEE PROFILE

Narayanarao Yathindra

Institute of Bioinformatics and Applied Biote…

80 PUBLICATIONS **1,218** CITATIONS

SEE PROFILE

Stereochemical Studies on Nucleic Acid Analogues. I. Conformations of α-Nucleosides and α-Nucleotides: Interconversion of Sugar Puckers via O4′-*exo*

Y. SWARNA LATHA and N. YATHINDRA*

Department of Crystallography and Biophysics, University of Madras, Guindy Campus, Madras, 600025, India

SYNOPSIS

The preferred conformations of ribo and deoxyribo α-nucleosides and α-nucleotides, the stereoisomers of the naturally occurring β-isomers, are worked out by minimizing the conformational energy as a function of all the major parameters including the sugar ring conformations along the pseudorotation path. The results of the studies bring out certain distinct conformational features that are at variance with their β counterparts. The range of glycosyl conformations are found to be not only quite restricted here but favor predominantly the *anti* conformation. The *syn* glycosyl conformation for the entire region of ℙ values are found to be energetically less favorable, with the barrier to *anti* ⇄ *syn* interconversion being higher especially in α-ribonucleosides. The energetically preferred range of pseudorotation phase angles (ℙ) is also considerably restricted and ℙ values corresponding to the C1′-*exo* range of sugars are highly unfavorable for α-nucleosides, in sharp contrast to the broad range of sugar ring conformations favored by β-isomers. While both *trans* ≃ 180° and *skew* ≃ 270° conformations around the C3′-O3′ (ϕ') bond are favored for α-3′-nucleotides with deoxyribose sugars, ribose sugars seem to favor only the *skew* values of ϕ'. Most interestingly and in sharp contrast to β-stereoisomers, an energy barrier is encountered at ℙ values corresponding to O4′-*endo* sugars. This suggests that the possible sugar pucker interconversion between C2′-*endo*/C3′-*exo* and C3′-*endo*/C2′-*exo* in α-anomers could take place only through the O4′-*exo* region. Likewise the possible path of *anti* ⇄ *syn* interconversion in α-nucleosides is not via high *anti*, in sharp contrast to β-nucleosides. These observations should be borne in mind while assigning the sugar ring conformers in α-nucleosides and those containing them from nmr investigations. Comparison of the results with β-anomers seem to suggest on the whole a lack of conformational variability or the restricted nature of α-stereoisomers. This could be one of the reasons for its nonselection in the naturally occurring nucleic acids.

INTRODUCTION

α-Nucleosides, the configurational isomer of the naturally occurring β-nucleosides, although not found in nucleic acids, are found to be constituents of naturally occurring small molecules such as α-nicotinamide adenine dinucleotide in *Azotobacter vinelandii*[1] and Vitamin B-12.[2] Some α-nucleoside 5′-phosphates act as substrates of 5′-nucleotidase[3,4] while α-5-formyluridine is found to be noncompetitive inhibitor of *Escherichia coli* DNA-dependent RNA polymerase.[5] α-Nucleosides and α-nucleotides are also shown to exhibit antiviral and antitumor activities.[6–10] More recently, oligo α-deoxyribonucleotides are shown to form complexes with strands containing complementary bases of either the α- or β-glycosyl linkage type,[11,12] and are found to have considerable importance in the study and understanding of gene regulation because of their ability to resist nuclease hydrolysis.[13–15] Thus, α-nucleosides and their polymers represent a unique class of biological molecular systems. Although it has been implied[11,12] that polymers of α-nucleosides form duplexes with themselves as well as with polymers of β-nucleosides, detailed stereochemical features characterizing them are lacking. Likewise the stereochemical factors responsible for their unusual behavior, especially the inhibiting action of nuclease digestion, are not known. With a view to elucidate above, we have taken up a systematic stereochemical

Biopolymers, Vol. 32, 249–269 (1992)

CCC 0006-3525/92/030249-21$04.00
* To whom correspondence should be addressed.

analysis of monomers and oligomers of α-stereomers. Here we report the results of detailed conformational energy calculations on monomers, which include nucleosides as well as 3′-nucleotides. The latter has been considered since 3′-phosphate, rather than 5′-phosphate, may exert influence on the preferred conformations of α-nucleotides because of its proximity to base. The results of the study show certain features that are distinctly different from the naturally occurring β-metabolites.

PROCEDURE

The entire range of sugar ring conformations as given by pseudorotation[16] as well as all the relevant exocyclic bond torsions are simultaneously considered in working out the energetically favored conformations of α-nucleosides as well as α-3′-nucleotides. The limited amount of x-ray data on α-anomers preclude a thorough analysis on the nature of variation of internal parameters of the furanose sugar ring as a function of $\mathbb{P}$. However, a comparison (Y. Swarna Latha and N. Yathindra, unpublished results) based on the limited set of data indicates that these values are nearly similar to those obtained for β-anomers.[17–19] Hence, the internal parameters recommended for β-anomers based on extensive analysis[17–19] have been adopted to obtain the coordinates of endocyclic and exocyclic atoms of the sugar ring for various values of $\mathbb{P}$ in α-stereochemistry. Furanose ring coordinates are generated for various values of $\mathbb{P}$ along the pseudorotation path based on the analytical procedure[20] for a constant value of amplitude of the sugar pucker $\tau_m = 39°$. Coordinates of the base and phosphate group are obtained using the standard geometry.[21] Hydrogen atoms of the sugar and the backbone are fixed on the basis of the tetrahedral arrangement. Similarly, coordinates of sugar ring along the pseudorotation path have been generated for $\tau_m = 20°$, adopting procedure similar to the above and by using regression coefficients reported in the literature[17] to account for variations of internal parameters as a function of τ_m. The notations used to define torsion angles are those suggested by Sundaralingam.[22] The zero value of glycosyl torsion (χ) corresponds to the *cis* conformation of the sequence of atoms O4′-C1′-N9(N1)-C4(C2). The χ angles in the range of 180° ± 90° and 0° ± 90° are referred to as *anti* and *syn* conformations, respectively, in accordance with IUPAC nomenclature.

The potential energy is estimated using the various contributions given in the following expression:

$$V_{total} = V_{Van\ der\ Waals} + V_{electrostatic} + V_{torsional} + V_{gauche} + V_{strain} \quad (1)$$

where

$$V_{Van\ der\ Waals} = \sum A_{ij}/r_{ij}^{12} - B_{ij}/r_{ij}^{6}$$

$$V_{electrostatic} = \sum 332 q_i q_j/\epsilon r_{ij}$$

$$V_{torsional} = \sum V_{3/2}^{[1+\cos(3\Phi)]}$$

$$V_{gauche} = \sum V_{2/2}^{[1+\cos(2\Phi)]}$$

$$V_{strain} = \sum K_0(\theta - \theta_0)^2$$

Here, K_0 is a force constant, and θ and θ_0 are, respectively, the actual and ideal value of a bond angle. Tetrahedral values are chosen for θ_0 as in earlier studies.[23,24] K_0 values of 40, 34, and 30 kcal/mol/rad^2 are taken for C—O—C, C—C—O, and C—C—C, respectively, to compute bond angle strain energy. Φ is the value of torsion angle, while V_2 and V_3 are the rotational barrier heights. Values of 2.5, 1.8, and 1.0 kcal/mol are used for V_3 in relation to rotations about the C—C, C—O, and P—O bonds, respectively. The *gauche* potential, V_{gauche}, is computed for the sugar ring using the parameters reported earlier.[23] Nonbonded van der Waals and electrostatic energy are computed for all pairs of nonbonded atoms separated by at least three intervening chemical bonds. The van der Waals interactions are calculated using the Lennard–Jones 6-12 potential function and the energy is minimized at $r_i + r_j + 0.2$, where r_i and r_j are the van der Waals radius corresponding to two atoms i and j, respectively. A_{ij} and B_{ij} are Lennard–Jones potential constants for a given pair of interacting atoms i and j, and r_{ij} is the distance between atoms i and j. The values of B_{ij} depend on the type of atoms i and j, and may be evaluated from atomic polarizabilities and effective number of valence electrons using the Slater–Kirkwood equation. A_{ij} can be evaluated[25] from B_{ij}. The q_i and q_j are the partial charges assigned to atoms i and j, respectively. Partial charges obtained earlier[26] by approximate molecular orbital theories are used to estimate electrostatic interaction energy with a dielectric constant ϵ of 4.

To facilitate a detailed understanding of conformational properties of α-nucleosides and α-nucleotides, two types of conformational energy maps are constructed, namely, ($\mathbb{P} - \chi$) and ($\mathbb{P} - \phi'$), where χ and ϕ' define the glycosyl and the exocyclic C3′— O3′ bond torsions, respectively. The torsions around all the other relevant exocyclic bonds are varied simultaneously for each combination of ($\mathbb{P}$

$-\chi$) and ($\mathbb{P}-\phi'$), and the final energy is computed corresponding to their minimum energy orientations. While the bond torsions are varied from 0° to 350° at intervals of 10°, the phase angles of sugar ring are varied at intervals of 18°. Isoenergy contours are drawn at intervals of 1 kcal/mol relative to the lowest minimum and contours greater than 5 kcal/mol are not shown, while contours of 0.5 kcal/mol are marked by dotted curves. Both ribose and deoxyribose sugars and a representative purine and pyrimidine base are considered. To facilitate comparison, calculations have also been performed for the corresponding β-anomers.

RESULTS AND DISCUSSION

Sugar Ring Conformations and Their Interconversion in α- and β-Nucleosides

To study the effect of α and β glycosyl C-N linkages (Figure 1) on the preferred range of sugar ring conformations, potential energies are calculated for both riboses as well as deoxyriboses (possessing the glycosyl C—N bond) for all the ring conformations along the pseudorotation path at an interval of 18°. Hence, nonbonded interactions that encompass atoms only up to N9(N1), C5′, O3′, and O2′/H2′ are considered, and interactions of atoms beyond the glycosyl nitrogen atom N (N1 in pyrimidines and N9 in purines) and C5′ of hydroxymethyl group (see Figure 1) are not included. The energy profiles thus obtained are shown in Figure 2. This calculation partially mimics the situation of a "free" sugar, although a glycosyl (C—N) bond instead of a glycosidic (C—O) bond exists in nucleoside sugars (other consequences of this such as absence/presence of anomeric effect are pointed out later). It can be seen from Figure 2 that the regions spanning the C2′-*endo* and C3′-*exo* range of puckers are most preferred in all cases, while regions covering C3′-*endo* and C2′-*exo* puckers are of higher energy and varies by nearly 0.7 to 1.5 kcal/mol depending on the type of sugar. The difference in energy between C3′-*endo* ($\mathbb{P}=18°$) and C2′-*exo* ($\mathbb{P}=342°$) regions for β-ribose is very small ($\simeq 0.25$ kcal/mol) while it is of the order of 1 kcal/mol for α-ribose. A distinct local minima also occurs in the C1′-*endo* region for α-ribose. This suggests that α-riboses especially may favor more C2′-*exo*/C1′-*endo* rather than C3′-*endo* range of conformations. Interestingly, an energy barrier near O4′-*endo* and C4′-*exo* regions (Figure 2) occurs for all the sugars, including those with β-glycosyl linkages, and is found to be mainly due to *gauche* effect and strain energy. The barrier height is about 2 kcal/mol in all cases, except in α-ribose, where it is around 3 kcal/mol. On the other hand, the barrier is less than 1 kcal/mol near C4′-*endo* and O4′-*exo* regions for all except for α-riboses. However, consideration of the characteristic nonbonded interactions between the other atoms of the base, especially those beyond the glycosyl nitrogen atom (see Figure 1), and the sugar alter this situation, resulting in higher energy barrier (Figure 3) at O4′-*exo* for β-sugars in nucleosides. The impor-

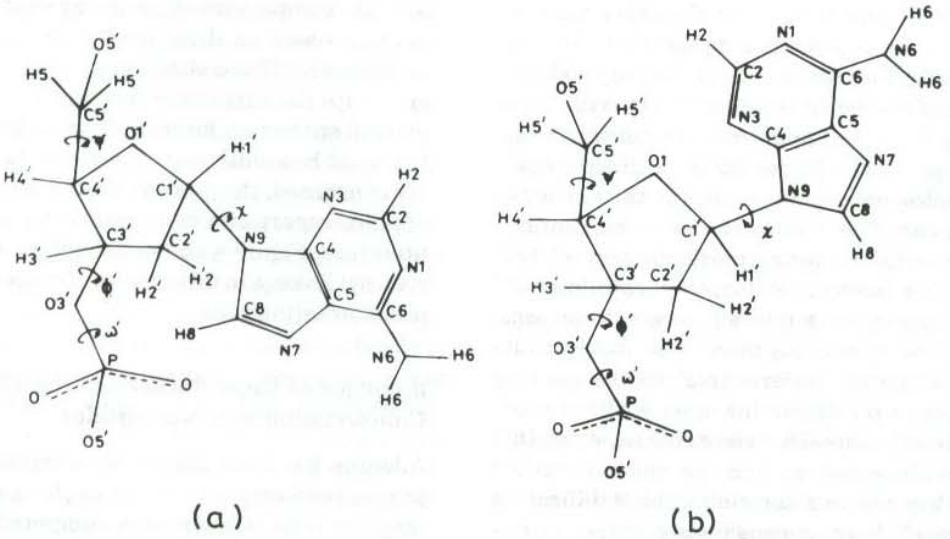

Figure 1. Schematic drawing of deoxyadenosine 3′-monophosphate with (a) α-glycosyl and (b) β-glycosyl linkage.

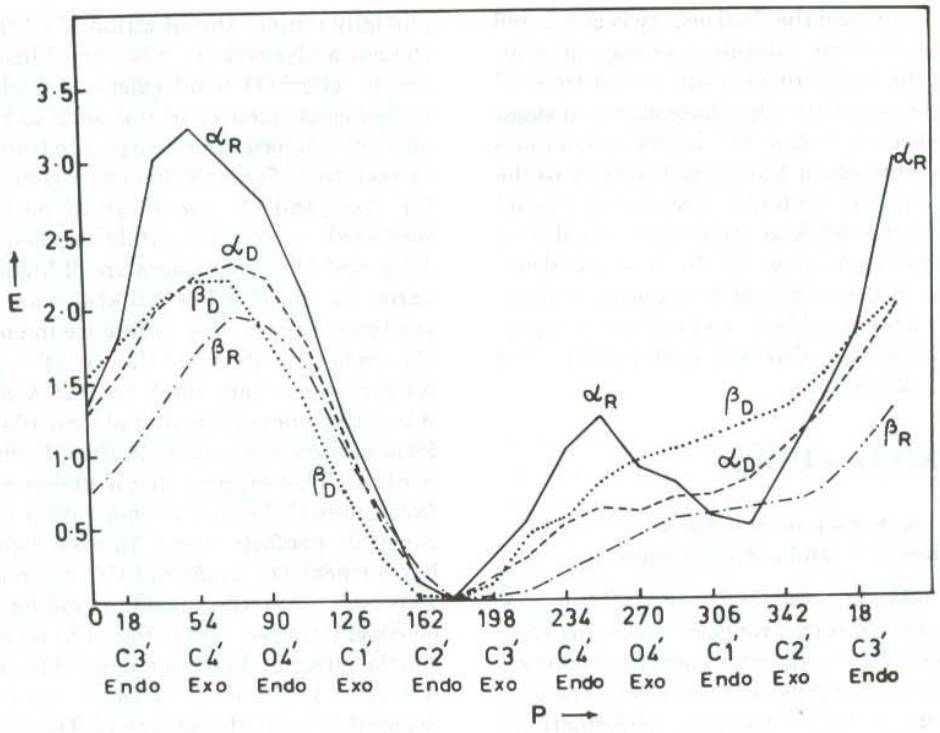

Figure 2. Variation of potential energy (E kcal/mol) for different types of *sugars with glycosyl* C-N linkage along the pseudorotation (ℙ) path: α_D (-----) α-deoxyribose; α_R (——) α-ribose; β_D (· · · · ·) β-deoxyribose, and β_R (– · – · –) β-ribose. Each curve represents energies relative to the global minimum obtained for the corresponding sugar. Nonbonded interactions beyond glycosyl nitrogen and C5′ atom of hydroxymethyl group are not considered (see text).

tance of nonbonded interactions in producing this characteristic barrier at the O4′-*exo* region has also been noted previously.[23,27–31] On the other hand, in the case of α-nucleosides it is found that the nonbonded interactions enhance the already existing barrier at the O4′-*endo* rather than at O4′-*exo*. These clearly bring forth the importance of atoms or groups beyond the glycosyl nitrogen atom in altering energetics of nucleoside sugars, especially the barrier to interconversion. One therefore has to be cautious about the conclusions, drawn particularly in relation to sugar pucker interconversion, from calculations[32] that do not incorporate relevant base interactions, or at least those mimicking them. The above results further show that the preferred regions of sugar ring conformations vary depending upon whether it occurs as a part of nucleoside or as a free sugar/methyl furanosides since factors like the anomeric effect that play a key role in determining the stabilization of free sugars[33–37] are conspicuously absent in nucleosides. Similarly, the additional nonbonded interactions due to appended atoms/groups (on the glycosyl nitrogen atom) that are found to be critical in nucleosides (see above) are absent in free sugars. A direct comparison of preferred sugar ring conformations based on these two results is therefore not appropriate. These observations are also in conformity with the earlier conclusions made from experimental studies on furanoses/methylfuranosides.[33–37] It should be mentioned that as far as α-nucleosides are concerned, the present study represents the first detailed report of a conformational analysis in the literature. Figure 4 shows deoxyribo sugars with α-glycosyl linkage in different conformations along the pseudorotation path.

Influence of Sugar Pucker on Glycosyl Conformation in α-Nucleosides

Adenine has been chosen as a representative of a purine base and a ($\mathbb{P}$ – χ) conformational energy map for α-deoxyadenosine computed according to procedures mentioned above, and is shown in Figure 5a. The global minimum occurs at ($\mathbb{P}$, χ) ≃ (162°,

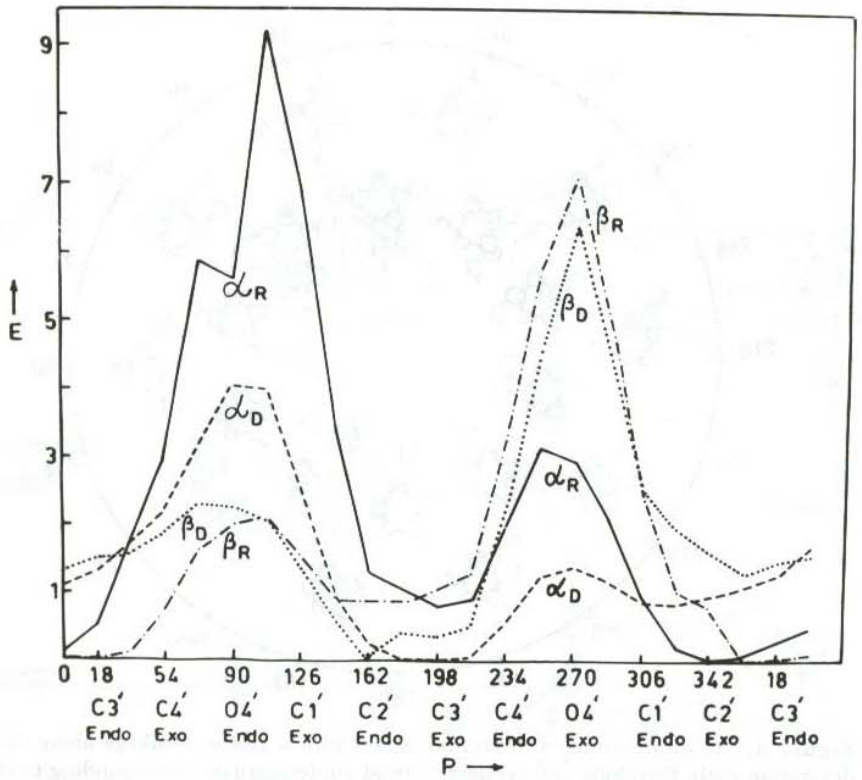

Figure 3. Variation of energy (E kcal/mol) for adenosine for different types of sugars along the pseudorotation (P) path: α_D (----) α-deoxyadenosine; α_R (——) α-adenosine; β_D (· · · ·) β-deoxyadenosine; and β_R (– · – · –) β-adenosine. Each curve represents energies relative to the global minimum obtained for the corresponding sugar. Energies corresponding to the most preferred conformations about the exocyclic bonds are considered.

170°) and the low energy region extends to cover C3′-*exo* and C4′-*endo* regions, while the energy sharply increases for the C2′-*endo* and C1′-*exo* range for all values of χ and especially for $\chi \simeq 180° \pm 40°$ in the *anti* region. This is due to steric interactions between the atoms of the base and the O3′, H4′, and C4′ atoms of the sugar. A secondary minimum that is higher by only 0.5 kcal/mol occurs, covering the C2′-*exo* and C1′-*endo* regions of the sugar pucker for χ values spanning 160° ± 30° in the *anti* region. On the other hand, *anti* glycosyl conformation for C3′-*endo* sugars turns out to be at least 1.5 kcal/mol higher in energy. This is mainly due to the high energy of C3′-*endo* sugars as discussed earlier (see Figure 2). The above results amply demonstrate that the preferred *anti* range of glycosyl conformations is strongly correlated to the nature of sugar ring conformation in α-nucleosides. Values of $\chi = 0° \pm 40°$ in the *syn* region turn out to be higher in energy by at least 1.5 kcal/mol for the entire range of sugar puckers due to the unfavorable interactions between the atoms C4 and N3 of the base and O4′ of sugar. Similarly, high *anti* ($\chi \simeq 300°$) conformations are rendered high energy due to the unfavorable interactions of the atoms C4 and N3 of base with C3′ and O3′ of sugar.

It should be noted that the χ values between 120° and 150° in the *anti* range are energetically highly unfavorable for sugars spanning P values in the range of 120° to 216° mainly because of the steric conflict of the O3′ atom of the sugar with C8 and H8 atoms of the purine base. Notice also the shift in the preferred *anti* range of glycosyl torsions to lower values (120°–180°) especially in the *anti* region, from the usual range (180°–240°) favored by β-nucleosides (Figure 5c). Unfavorable interactions of N3 and C4 atoms of the base with C2′ and H2′ atoms of the sugar are primarily responsible for this shift. Overall one can readily observe, by comparison with the corresponding β-nucleosides (Figure 5c), that the glycosyl torsions are significantly restricted in α-nucleosides (Figure 5a) and the favored range is correlated to the type of sugar ring conformation.

It is noteworthy that the O4′-*exo* region separat-

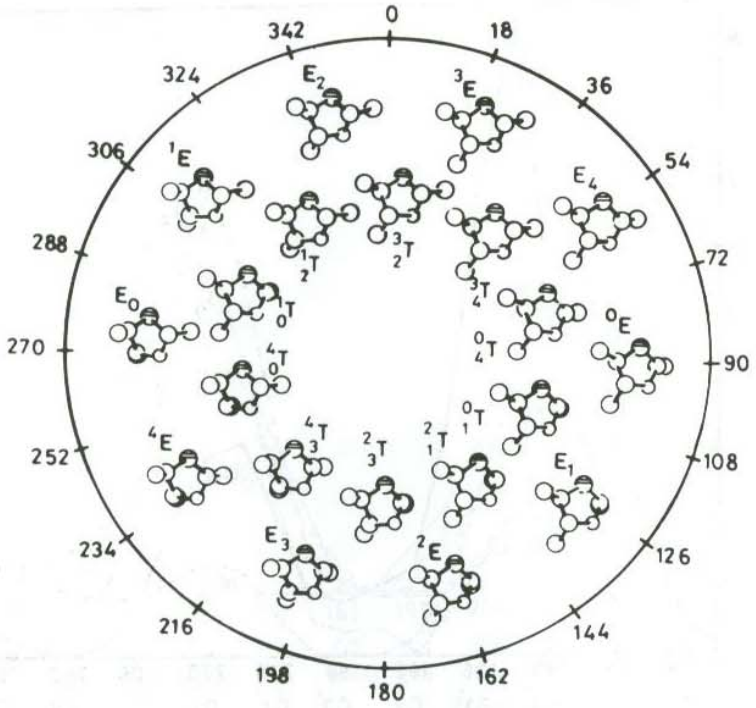

Figure 4. Conformations of deoxyribo sugars with α-glycosyl linkage along the pseudorotation path. Envelope and symmetric twist conformations corresponding to the amplitude of pucker $\tau_m = 39°$ are shown along the outer and the inner circles, and are labeled. The O4′ atom of each of the sugar rings is shaded for easy identification of other ring atoms. Values of phase angles ($\mathbb{P}$) in multiples of 18° are marked.

ing the C2′-*exo* and C3′-*exo* range of the sugar ring conformation in α-nucleosides (Figure 5a) has only a small barrier compared to a higher barrier near the O4′-*endo* separating the C3′-*endo* and C2′-*endo* sugars. Highly unfavorable steric interactions of the C4′ and H4′ atoms of the sugar with the atoms of the base render the O4′-*endo* domain of the sugar ring conformation energetically less likely. Admittedly, then, the possible interconversion in α-stereoisomers should necessarily occur via O4′-*exo* rather than O4′-*endo*. Similarly, the presence of a large barrier for χ values in the range of 210°–300° in sharp contrast to results found in the corresponding β-nucleoside (Figure 5c) readily suggest that the possible path of *anti* $\rightleftarrows$ *syn* interconversion in α-isomers is different (via $\chi \simeq 100°$) and does not occur via the so-called high *anti* ($\chi \simeq 300°$) conformation. These are some of the most striking differences in the conformational behavior of α- and β-nucleosides.

Similar calculations with ribose sugars (Figure 5b) suggest even greater restrictions to the glycosyl rotations with the overall features being nearly similar. It can be seen that the global minimum now shifts to the C2′-*exo* domain, indicating a preference for a C2′-*exo-anti* conformational combination, although the C3′-*exo-anti* conformation is only 0.5 kcal/mol higher in energy. This shift of the global minimum from the C3′-*exo* to the C2′-*exo* region as the sugar is changed from deoxyribose to ribose is related to the additional small stabilizing interactions between the substituent at C2′ and the base. On the other hand, the energy barrier at O4′-*endo* is further enhanced for α-adenosine due to enhanced steric interactions introduced by the O2′ hydroxyl group. Because of this, a higher energy barrier is found here for possible *anti* $\rightleftarrows$ *syn* as well as sugar ring interconversion compared to α-deoxyribonucleosides (Figure 5a). The variation in bond angles by a few degrees, especially at the glycosyl nitrogen atom viz. C1′-N9-C4/C1′-N1-C2 and C1′-N9-C8/C1′-N1-C6 from their average values of 126°/117° and 128°/121.5°, respectively, essentially leads to similar results besides retaining the energy barrier at O4′-*endo*. Comparison with ($\mathbb{P} - \chi$) maps (Figure 5d) obtained for the corresponding β-stereomers readily reveals significant conformational restriction in α-isomers.

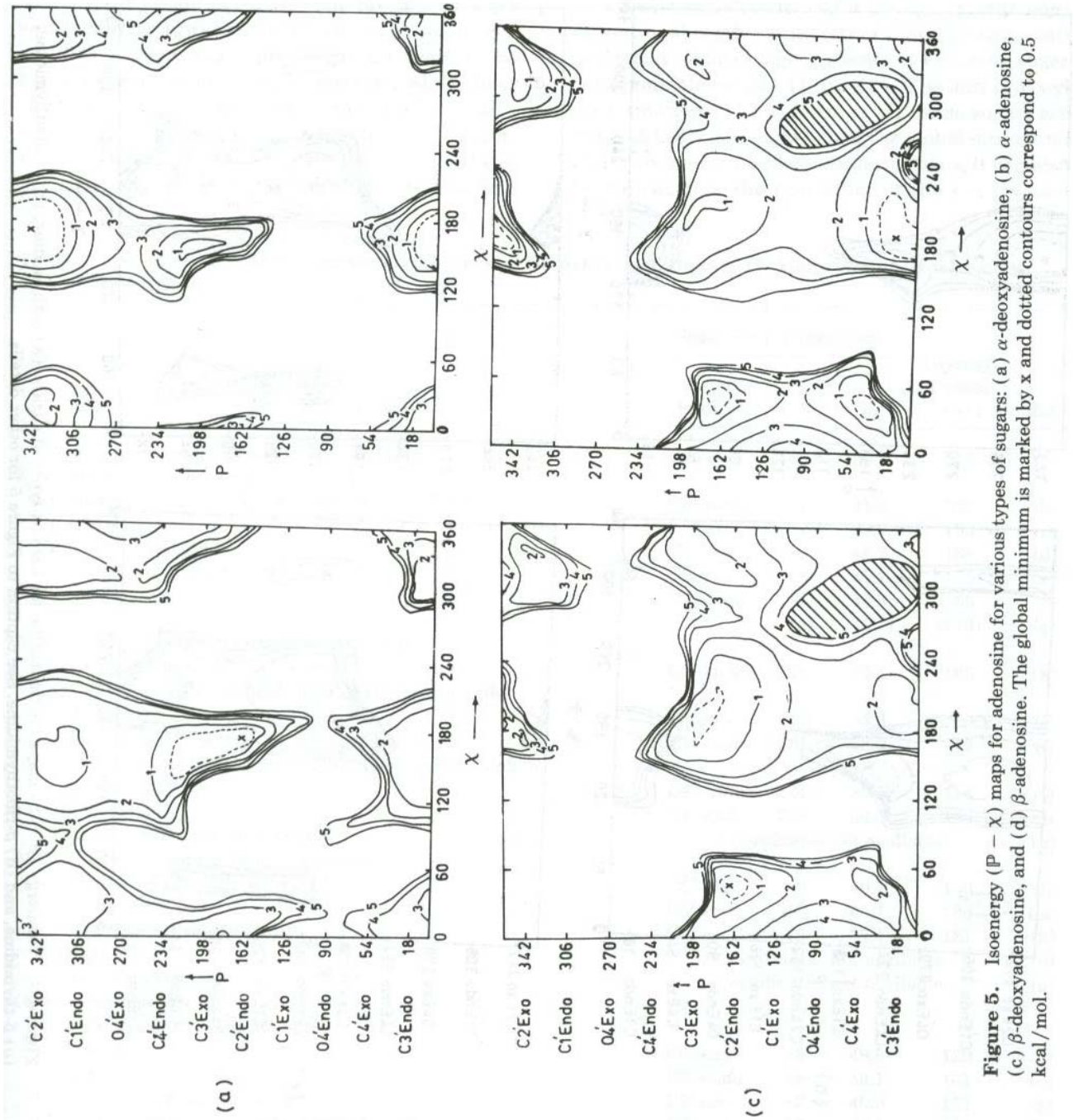

Figure 5. Isoenergy ($\mathbb{P} - \chi$) maps for various types of sugars: (a) α-deoxyadenosine, (b) α-adenosine, (c) β-deoxyadenosine, and (d) β-adenosine. The global minimum is marked by x and dotted contours correspond to 0.5 kcal/mol.

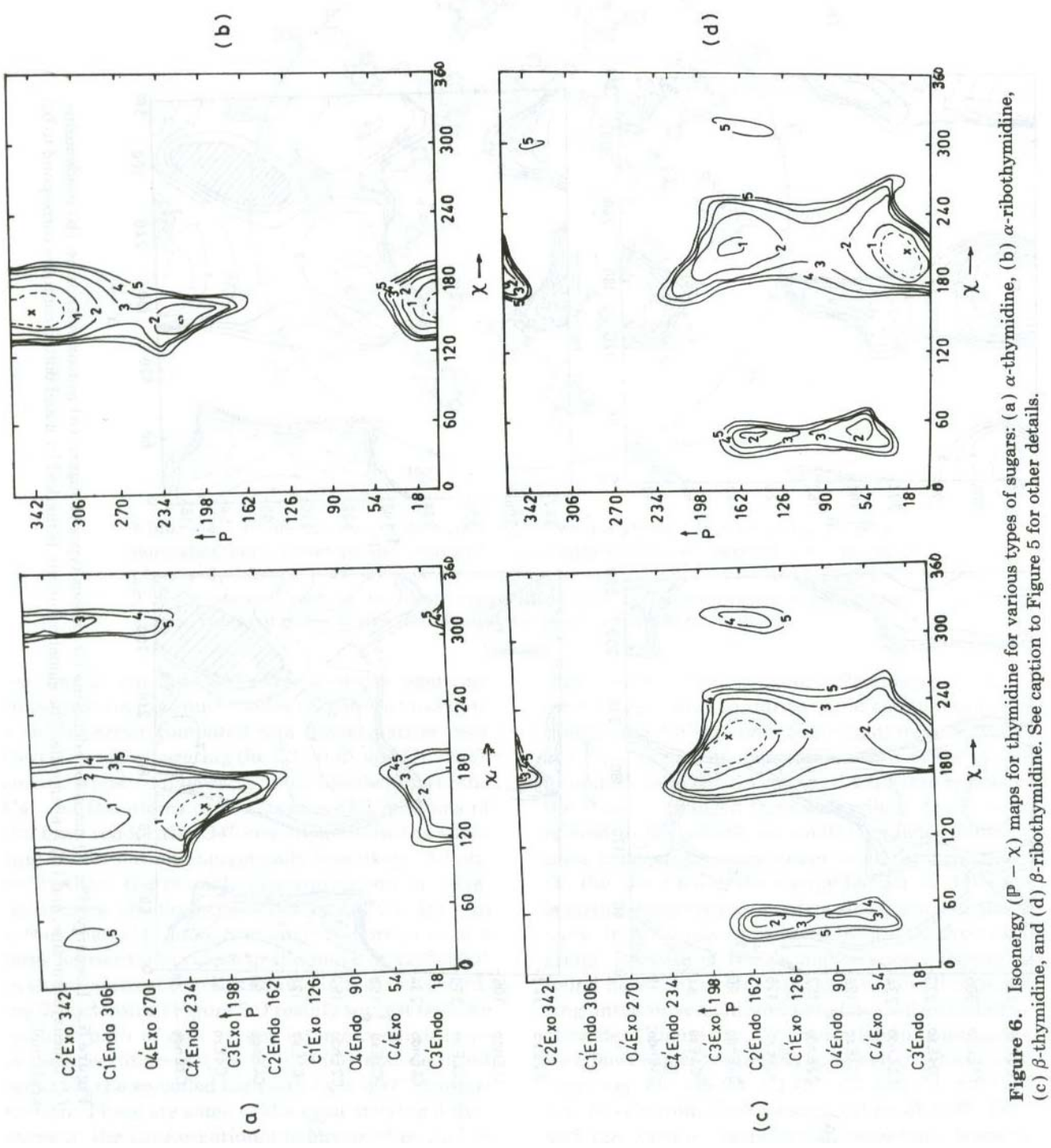

Figure 6. Isoenergy (P − χ) maps for thymidine for various types of sugars: (a) α-thymidine, (b) α-ribothymidine, (c) β-thymidine, and (d) β-ribothymidine. See caption to Figure 5 for other details.

Conformational energies computed similar to the above for α-thymidine, which is chosen as a representative of α-deoxypyrimidine nucleosides, are shown in Figure 6a. It can be readily seen, as expected, that glycosyl rotations are even more restricted for pyrimidines and also compared to its β-counterpart (Figure 6c). Low energy contours are shifted further toward higher P values between 180° and 234°, suggesting a preference for the C3′-*exo* and C4′-*endo* region of sugar puckers, while those covering P values that range from 126° to 180°, which include the C1′-*exo* and C2′-*endo* conformations, are rendered relatively high energy states in sharp contrast to β-thymidine (Figure 6c). In fact, all the known α-deoxyribonucleosides exhibit these preferred sugar conformations (Table I and Figure 7). The shift toward the low *anti* region seen here is similar to that found in purines, and is due to the unfavorable steric interactions of C6 and H6 with O3′, and C2 and O2 with C2′ and H2′ atoms involving base and sugar. Preference for the C3′-*exo-anti* conformational combination rather than C3′-*endo-anti* is clear. A slightly higher energy of C3′-*endo* sugar is responsible for this (Figure 2). The *anti* glycosyl conformations with C2′-*exo* or C1′-*endo* sugars are only 0.5 kcal/mol higher than the global minimum, and represent other likely conformations. It can also be noticed that the possibility of the *syn* glycosyl

Table I Conformational Parameters from Crystal Structures of Molecules Comprising α-Nucleosides and α-Nucleotides

Crystal Structure	Sugar Ring Parameters[a]			Glycosyl Torsion	Ref.[c]
	Sugar Pucker	P (°)	τ_m	χ (°)	
α-D-2′-Amino-2′-deoxyadenosine monohydrate	C3′-*exo*	188	30.3	115	(a)
Molecules comprising α-ribopurines					
5,6-Dimethyl-1-(α-D-ribofuranosyl)-benzimidazole	C3′-*endo*	12	41.6	322	(b)
Vitamin B_{12} (wet)	C2′-*exo*	−17	49.1	133	(c)
Vitamin B_{12} (air dry)	C2′-*exo*	−10	48.2	138	(d)
Vitamin B_{12} 5′-phosphate	C2′-*exo*	−8	47.1	135	(e)
Vitamin B_{12} coenzyme	C3′-*endo*	19[b]	43.9	155	(f)
		(5)	(49.2)	(140)	(g)
Molecules comprising α-deoxyribopyrimidines					
α-5-Acetyl-2′-deoxyuridine	C2′-*endo*	168	34.4	166	(h)
5-[1-(2′-Deoxy-α-D-ribofuranosyl)uracilyl] disulphide					
Molecule 1	C3′-*exo*	184	35.3	150	(i)
Molecule 2	C4′-*endo*	219	28.0	115	(i)
5-[1-(2′-Deoxy-α-D-ribofuranosyl)uracilyl]methylsulphide					
Molecule 1	C4′-*endo*	224	30.8	114	(j)
Molecule 2	C4′-*endo*	219	34.5	128	(j)
5-Fluro-2′-deoxy-α-4′-thiouridine	Coordinates not available				(k)
Molecules comprising α-ribopyrimidines					
α-Cytidine	C2′-*exo*	−3	40.1	158	(l)
α-5-Formyluridine	C3′-*endo*	17	40.1	163	(m)
α-Pseudouridine monohydrate	C2′-*exo*	−18	37.1	181	(n)
α-Thymidine	Coordinates not available				(o)
α-D-O-2-2′-Cyclouridine	Coordinates not available				(p)
Other α-nucleosides					
9-α-D-Arabinofuranosyl-adenine					
Molecule 1	C2′-*exo*	−5	49.5	120	(q)
Molecule 2	C3′-*endo*	18	39.1	101	(q)
1-α-D-Xylofuranosyl-cytosine	C2′-*exo*	−3	40.9	157	(r)
1-α-D-Xylofuranosyl-cytosine hydrochloride	C3′-*endo*	16	38.8	158	(r)
4-(α-D-Arabinofuranosyl)-imidazo[4,5,-C]-4,5,6,7-tetrahydropyridine	C3′-*endo*	9	36.4	174	(s)

[a] P is the phase angle of pseudorotation and τ_m is the amplitude of sugar pucker.
[b] From latest data.
[c] See Appendix A.

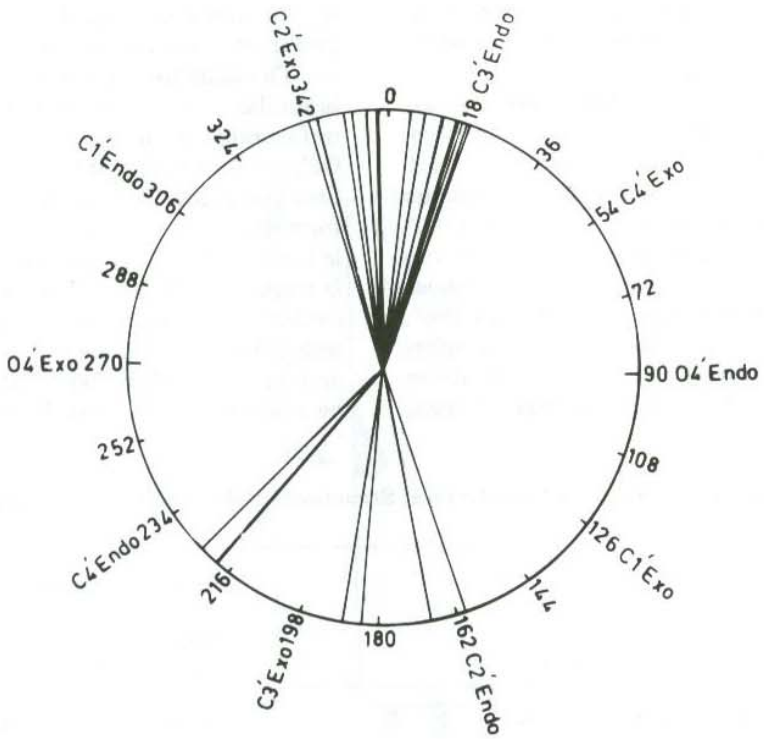

Figure 7. Phase angles of pseudorotation of α-sugars found in different crystal structures of nucleosides and nucleotides.

conformation, although of much higher energy, is associated with C2′-*exo*/C1′-*endo* and not C2′-*endo*/C3′-*exo* sugar puckers. This is in accord with the observation from nmr studies[38] on nucleosides where a decrease in C2′-*endo* population concomitant with an increase in C3′-*endo* population is found when the C6 substituted base is forced into a *syn* glycosyl conformation. The high energy barrier found (Figure 6a) near the O4′-*endo* is due to overwhelming steric interactions between the base and sugar caused due to the proximity of the six-membered ring with sugar.

Calculations performed with α-ribothymidines (Figure 6b) show that they exhibit higher overall restrictions compared to α-thymidine (Figure 6a), with the exception that the energetically most stable conformation now corresponds to C2′-*exo*-*anti*, suggesting the preference of C2′-*exo* sugars by α-ribopyrimidine nucleosides similar to α-ribopurines (Figure 5b). The *anti* range of glycosyl conformation is further reduced here due to additional unfavorable interactions introduced by the substituent at C2′. The *syn* and the high *anti* glycosyl conformations are rendered energetically even more unlikely compared to α-thymidine. The restricted conformational feature of α-ribothymidine can be seen by comparing with the corresponding β-nucleoside (Figure 6d).

The ($\mathbb{P} - \chi$) maps obtained for β-nucleosides are not discussed since they have already been described many times over, and are shown here only to highlight the significant differences in the conformations between α- and β-nucleosides. The features present in the maps of β-anomers, including the occurrence of global minimum and other local minima, however, are very similar to those obtained earlier.[27,29] The narrow range of preferred *anti* glycosyl conformation (χ) for α-anomers (Figures 5a, 5b, 6a, and 6b), in contrast to the fairly broad range of *anti* favored by β-anomers (Figures 5c, 5d, 6c, and 6d), is quite distinct, especially for purines, with both ribo and deoxyribo sugars. The shift of χ to lower values in the *anti* range is prominent in α-anomers for both purines and pyrimidines irrespective of whether the sugar is of ribo and deoxyribo type, while for β-anomers, χ values (in the *anti* range) shift to higher values. The range of *anti* χ values for C2′-*endo*/C3′-*exo* sugars is quite narrow while it is quite broad for C2′-*exo*/C3′-*endo*. This feature is in contrast to that found in the corresponding β-nucleosides. While β-nucleosides especially purines favor *anti*, high *anti*,

and even *syn* glycosyl conformations, α-anomers tend to favor exclusively the *anti* conformation. The paths for glycosyl *anti* $\rightleftarrows$ *syn* and sugar pucker C3′-*endo*/C2′-*exo* $\rightleftarrows$ C2′-*endo*/C3′-*exo* interconversions in α-nucleosides are quite different from those of β-nucleosides.

Table I lists the conformational parameters of all the structures containing α-nucleoside and α-nucleotide determined by x-ray crystallography. It is clear from Table I that except for one, all the nucleosides have their bases in the *anti* conformation, in excellent agreement with the observations from present study. A few nucleosides assume low *anti* χ values, outside the theoretically predicted range. It is found that in these situations τ_m values are quite low ($\simeq 30°$). The flattening of the ring due to low τ_m (small displacement of puckered atoms from mean plane) and consequent increase in separation between the involved atoms decreases the unfavorable nonbonded interactions enabling low values of χ to be favored. These interactions become severe at higher values of τ_m, leading to a narrow range of χ values, as seen in Figure 5a and discussed above. More details of the effect of τ_m on the favored glycosyl conformations are discussed in the section that appears later. In good agreement with the calculations, meager crystal structure data represented in Figure 7 show that C3′-*exo*/C4′-*endo* and C2′-*exo* conformations seem to be the preferred modes of sugar pucker in α-anomer. This is also in agreement with the earlier observation of Sundaralingam.[39] The nmr studies[38,40,41] on α-nucleosides and α-nucleotides have generally interpreted the results in terms of either the C2′-*endo* or C3′-*endo* conformation since it is extremely difficult to distinguish subtle variations in $\mathbb{P}$ leading to slightly different sugar ring conformations especially, within the broad ranges of ^{2}E and ^{3}E. The observation that a barrier to possible ^{3}E $\rightleftarrows$ ^{2}E interconversion occurs at O4′-*endo* rather than O4′-*exo* together with other features that became apparent from the present study must be taken into account in estimating the nature and population of sugar ring conformation of α-anomers from nmr studies.

Influence of Phosphate on α-Glycosyl Conformation

Because of the configurational isomerism at C1′, α-3′-nucleotides seem to mimic β-5′-nucleotides especially in relation to the proximity of base and phosphate. Hence, it is felt important to examine the phosphate effect on the favored glycosyl and the C3′— O3′ bond conformations in α-3′-nucleotides. The above calculations have therefore been repeated by including 3′-phosphate. The ($\mathbb{P} - \chi$) map computed for α-3′-deoxyadenosine monophosphate (α-3′-dAMP) and others are given in Appendix B (Figures A1 and A2). The nature of the energy map (Figure A1a) is very similar to that obtained for α-deoxyadenosine (Figure 5a) and 3′-phosphate does not bring in any additional steric constraint on the χ values. However, it seems to influence the preferred range of sugar as well as glycosyl conformations. The *anti* region of χ for the C3′-*exo* sugars are rendered energetically most preferred by nearly 1.5 kcal/mol compared to C2′-*exo* and C3′-*endo* due to additional favorable van der Waals interactions between the phosphate and the adenine base. Absence of these due to the distal nature of phosphate and base renders the C2′-*exo*-*anti* domain to be energetically less favorable compared to the situation in the corresponding nucleoside (Figure 5a). Other features in the ($\mathbb{P} - \chi$) maps are relatively unaffected by the phosphate.

Calculations on α-3′-AMP (Figure A1b) yield essentially similar results as that of the corresponding ribonucleoside (Figure 5b), except that the global minimum is now shifted to C3′-*exo*-*anti* due to the additional favorable base . . . phosphate interactions mentioned above. This results in a similar preference by both C2′-*exo* and C3′-*exo* regions of sugar for *anti* base.

Calculations (not shown) performed on α-3′-GMP showed that both *anti* and *syn* glycosyl conformations are nearly equally favored. The *syn* conformation in association with C3′-*exo* sugars are found to be particularly favored due to additional stabilizing interactions between the amino group of the guanine base and 3′-phosphate. This situation is somewhat similar to the behavior of guanine found in β-5′-GMP.[42]

The ($\mathbb{P} - \chi$) map obtained for α-3′-TMP (Figure A2a) have similar features of the corresponding nucleoside (Figure 6a). The already high energy *syn* and high *anti* regions are rendered even higher by the presence of phosphate. Similarly, C3′-*endo*-*anti* conformation combination in α-3′-TMP is nearly 2.5 kcal/mol higher compared to C2′-*endo*-*anti*. This is in contrast to β-3′-TMP (Figure A2c) where C3′-*endo*-*anti* tends to be the most preferred region. These differences arise mainly due to the energies of α- and β-glycosyl linked sugars, as discussed earlier. Stereo plots of α-3′-nucleotides for a few different sugar ring puckers including the favored C3′-*exo* sugar ring and *anti* glycosyl conformations are shown in Figure 8 for representative purine and pyrimidine bases. The largest and the smallest separation between the H4′ atom of sugar and the C8

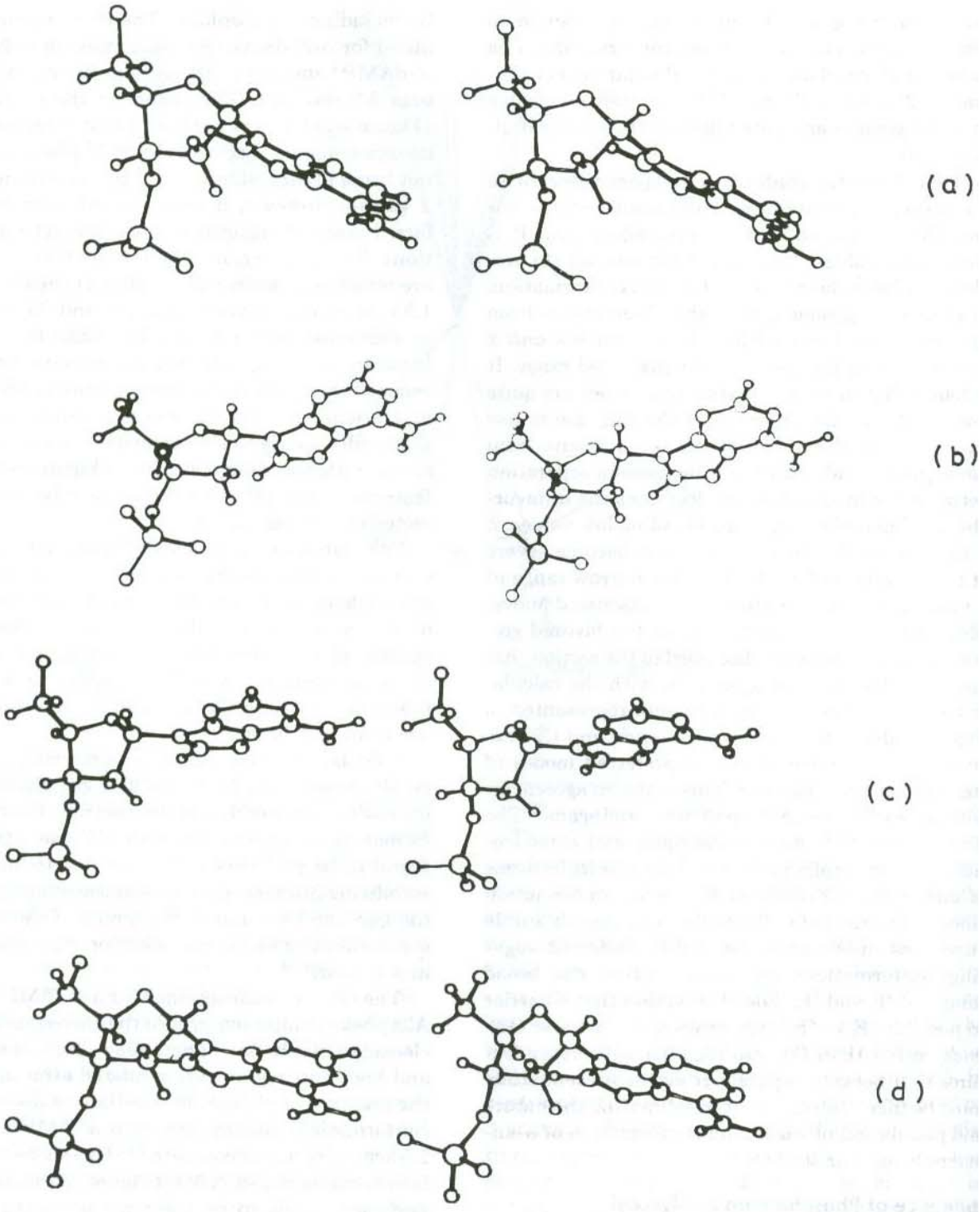

Figure 8. Stereo plots of α-3′-dAMP for a few selected sugar ring conformations (a) C3′-*exo*, (b) C2′-*exo*, (c) O4′-*exo*, and (d) O4′-*endo* and of α-3′-TMP (e) C3′-*exo*. Note that the base atoms are proximal to sugar ring atoms in (d) and distal in (c), in sharp contrast to β-sugars.

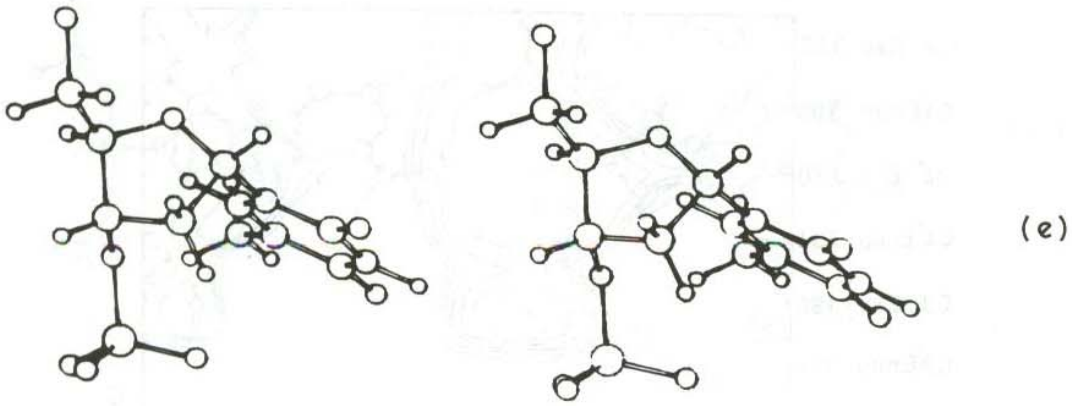

Figure 8. (*Continued from the previous page*)

and H8 atom of base in the O4′-*exo* and O4′-*endo* sugar puckers are clearly seen in Figure 8c and d, respectively. These are exactly opposite to those found in β-nucleotides.[43] These are the interactions responsible for the difference in the barrier locations for sugar ring interconversion in α- and β-nucleotides.

Calculations on α-3′-rTMP (Figure A2b) show features similar to α-3′-AMP (Figure A1b), with global minimum being shifted to C3′-*exo*-*anti* due to additional favorable base . . . phosphate interactions mentioned above. However C2′-*exo*-*anti* has energy similar to the global minimum. Other features in the map are analogous to that noticed in nucleoside (Figure 6b). Additional phosphate . . . base interactions restrict the preferred range of sugar as well as glycosyl conformations in 3′-pyrimidine nucleotides compared to corresponding nucleosides.

Influence of τ_m on the Favored Sugar and Glycosyl Conformations in α-Nucleotides

An interesting observation from Table I is that α-anomers exhibit a fairly large range (28°–50°) of τ_m compared to β-anomers, although the average value corresponds to 39°, similar to that found in β-anomers. Further, α-ribonucleosides tend to possess consistently higher value of τ_m than α-deoxyribonucleosides. Occurrence of higher τ_m concomitant with C3′-*endo*/C2′-*exo* sugar pucker ensures larger separation between base and the axially disposed O2′ atom, thus overcoming the possible steric interactions between them. On the other hand, it accentuates unfavorable steric interactions with other sugar atoms such as O3′, H4′, and C4′ favoring low *anti* glycosyl torsions especially for C2′-*endo* sugars. Low τ_m values alleviate these interactions. In order to examine these and other effects, as well as to explain the experimentally observed low values of χ in some α-anomers, representative calculations similar to those above have been performed for α-dAMP with a low value of τ_m ($\simeq 20°$) for the sugars. The ($\mathbb{P} - \chi$) conformational map thus obtained is shown in Figure 9. It can be clearly seen that the lowest energy sugar puckers correspond to C3′-*exo* and C4′-*endo* while all the other sugar puckers turn out to be higher energy conformations. In fact, all the experimentally observed sugars (Table I) exhibiting low τ_m have either C4′-*endo* or C3′-*exo* sugar puckers, in excellent agreement with the results of present calculations. Further, low values of *anti* glycosyl conformations, $\chi < 150°$ that are sterically prohibited in α-3′-dAMP (Figure A1a) are now favored, thus also explaining why a few nucleosides possessing low τ_m are found to have low χ values. Stereo plots of α-3′-dAMP possessing the C3′-*exo* sugar pucker with τ_m values of 20° and 39° are shown in Figure 10 to illustrate the effect of τ_m especially on the energetically favored glycosyl conformation.

Influence of α-Linkage on C3′-O3′ Torsion

Because of the proximity of 3′-phosphate and α-base, it is also felt important to examine their mutual influence on the preferred conformations as a function of sugar ring pucker. A ($\mathbb{P} - \phi'$) conformational map provides a description of this. Such a map obtained in α-3′-dAMP is shown in the Figure 11a. The global minimum occurs at ($\mathbb{P}$, ϕ') = (198°, 200°). A low energy region of similar magnitude also spans $\phi' \simeq 270°$. Both these regions favor sugar puckers ranging from C2′-*endo* to C3′-*exo*, while the C1′-*exo* range of sugar pucker is not favored. The familiar C3′-*endo* region is rendered high energy by about 1.5 kcal/mol even for $\phi' \simeq$ *trans* due to the absence of additional favorable interactions between base

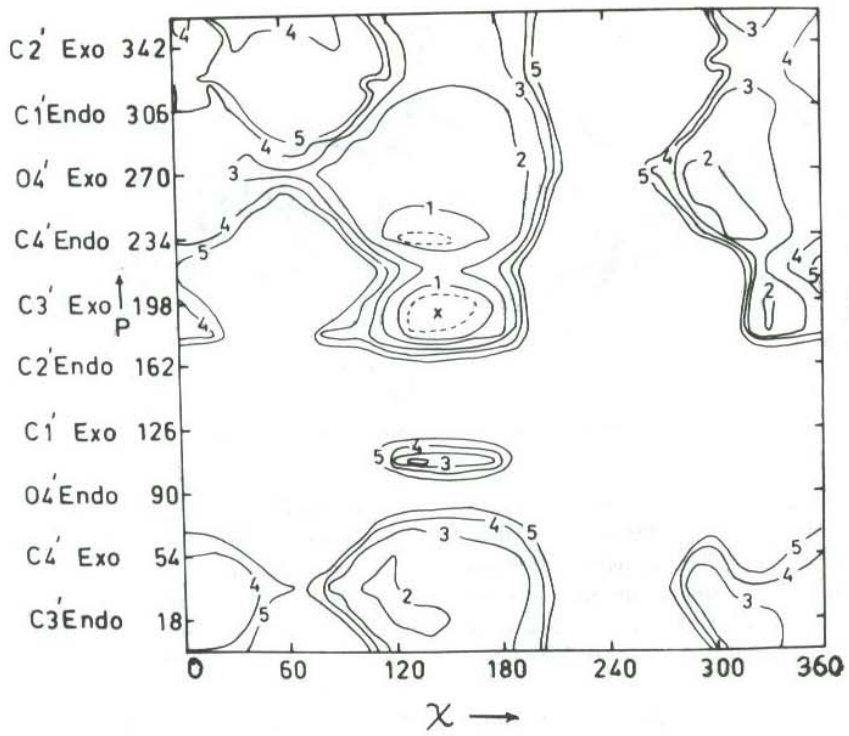

Figure 9. Isoenergy ($\mathbb{P} - \chi$) map for 3′-dAMP at $\tau_m = 20°$. Note the distinct changes in preferred ranges of glycosyl as well as sugar ring conformations (see text). See caption to Figure 5 for other details.

and 3′-phosphate and the high energy of C3′-*endo* sugars. This is in contrast to β-nucleotides (Figure 11c), where *trans* ϕ' values are nearly equally favored for both C3′-*endo* and C2′-*endo* sugars because of the conspicuous absence of sugar pucker dependent base . . . 3′-phosphate interactions as well as the fact that the difference in energy between C3′-*endo* and C2′-*endo* sugars in β-D-sugars is negligible (Figure 2). These are in fine agreement with observations[44,45] from crystal structure data on DNA oligomers that exhibit both *skew* and *trans* values of ϕ' concomitant with C2′-*endo* puckers for sugars.

As is well known,[22,28,46] the *skew* domain of ϕ' for $\mathbb{P}$ values corresponding to the C3′-*endo* domain of sugar puckers is of higher energy due to the unfavorable interactions between C5′, O5′, H5′, and H′5 atoms of sugar and the phosphate group. The energy barrier near the O4′-*endo* region (Figure 11a) instead of O4′-*exo*, a characteristic of α-nucleotides, is brought out here also. These results demonstrate that while α-base glycosyl linkage does not sterically influence ϕ' torsions or its range, it influences the preference of C3′-*exo* rather than C3′-*endo*/C2′-*exo* sugars for both *trans* and *skew* values of ϕ'.

Similar calculations on α-3′-AMP (Figure 11b) with ribose sugars show that values of $\phi' \simeq 270°$ are strongly favored for both the C2′-*endo* and C2′-*exo* ranges of sugar puckers, while the $\phi' \simeq$ *trans* region represents the high energy conformation by 2–3 kcal/mol even for C3′-*exo*/C2′-*endo* sugars. This high energy arises due to the unfavorable van der Waals repulsive interactions between the substituent at C2′ and the phosphate group, and this feature is similar to that noticed for β-3′-AMP (Figure 11d). The energy difference between C3′-*endo* and C2′-*exo* puckers in ribose sugars with α-glycosyl linkage as discussed earlier (see also Figure 2) renders the C3′-*endo* region unfavorable by nearly 1.5 kcal/mol for *trans* ϕ'. On the other hand, absence of these in β-anomers renders both the C3′-*endo* and C2′-*exo* conformations equally likely. It is also seen from comparison that β-3′-ribonucleotides (Figure 11d) strongly favor the C3′-*endo*-*trans* conformational combination. The *skew* conformation of ϕ' even for C2′-*endo* sugars in β-3′-ribonucleotide (Figure 11d) is of higher energy by 1.5 kcal/mol. This feature is in contrast to that seen in β-deoxyribonucleotides (Figure 11c) where both these regions are nearly

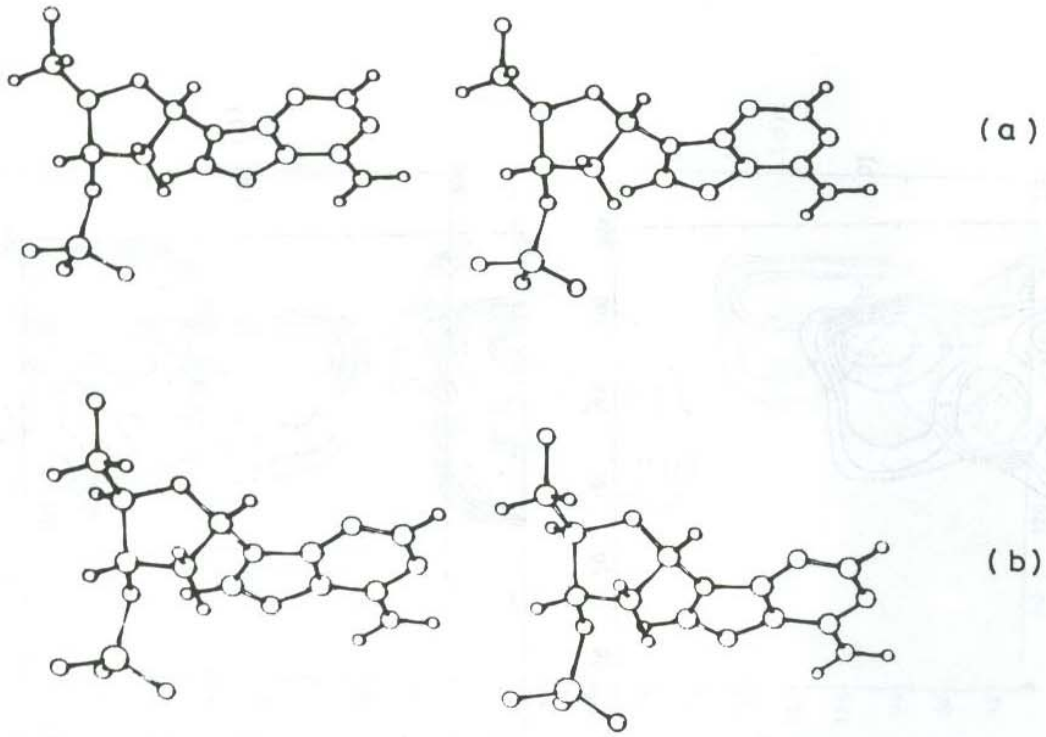

Figure 10. Comparison of molecular conformation of α-3′-dAMP at two different amplitudes of sugar pucker (a) $\tau_m = 20°$ and (b) $\tau_m = 39°$ for the C3′-*exo* sugar pucker with $\chi = 120°$. Note the proximity of H8 atom of adenine with O3′ atom of sugar in (b) compared to (a). This interaction prevents the base from assuming χ values in the range of 100°–140° in (b).

equally favorable. These suggest that $\phi' \simeq$ *trans* is strongly favored by β-riboses concomitant with C3′-*endo* sugars. These results on β-3′-nucleotides are generally similar to the earlier work[28,32,47] except that the $\phi' \simeq$ *trans* region is also rendered low energy conformation when the fixed C2′-*endo* sugar ring conformation is considered for the ribose sugar.[47]

Studies on α-3′-TMP (Figure 12a) show a preference to the *trans* value of ϕ', with $\phi' \simeq$ *skew* being higher by only 0.5 kcal/mol for C3′-*exo* puckers. Regions corresponding to $\phi' \simeq$ *trans* for the C2′-*endo* sugar pucker is rendered high energy by 1.0–1.5 kcal/mol and 2.5 kcal/mol for C3′-*endo*/C2′-*exo* sugars. Both these features are slightly at variance compared to β-3′-TMP (Figure 12c) and arguments presented above in relation to α-3′-dAMP (Figure 11a) may be used to explain this.

Calculations on α-3′-rTMP (Figure 12b) reveal essentially similar features as seen in the case of α-3′-AMP (Figure 11b). Comparison of these with β-3′-rTMP (Figure 12d) brings forth similar differences that are noticed between α-3′-AMP and β-3′-AMP (Figure 11).

CONCLUSIONS

Conformational studies on α-nucleosides and their 3′-nucleotides reveal important differences in their conformational behavior in relation to the preference of sugar ring conformations as well as their influence on the favored glycosyl conformations. There is a clear trend for the preference of C3′-*exo*, C4′-*endo*, and C2′-*exo* regions of sugar pucker in α-isomers. Distinct preference for C3′-*exo* has recently also been noted for sugars from nmr studies on α-deoxyoligonucleotides.[15] While C4′-*endo* sugars become important for α-sugars, C1′-*exo* puckered rings turn out to be higher energy conformations. Even C2′-*endo* sugars are not energetically favored for α-pyrimidine nucleosides especially with riboses. These observations are in excellent agreement with the limited x-ray data on α-anomers. The most striking difference has been the occurrence of a barrier to sugar ring interconversion at O4′-*endo* in α-sugars, in contrast to O4′-*exo* found in β-sugars. Surprisingly, no observation on this aspect has been made earlier in any of the nmr studies,[15,38,40,41] al-

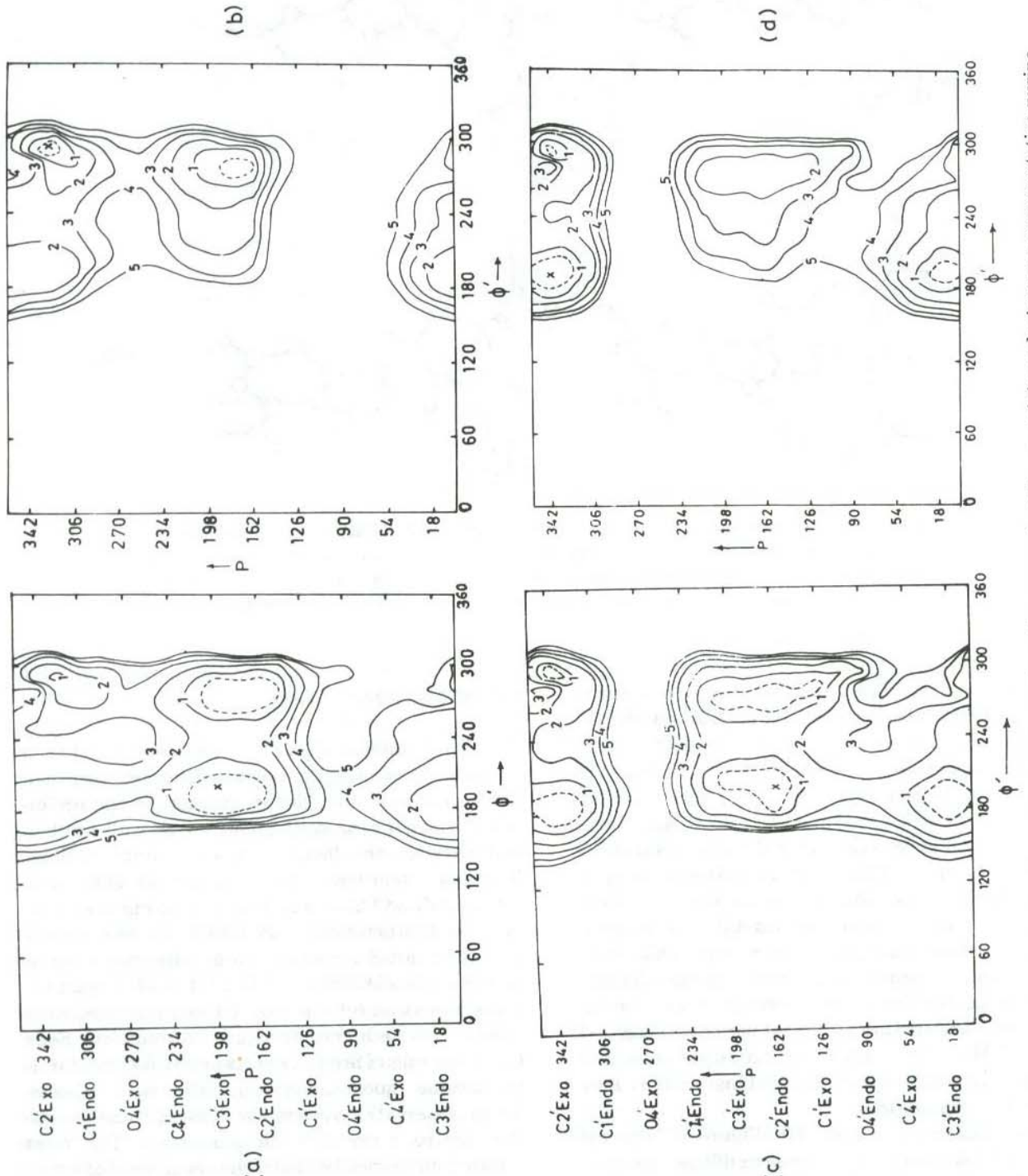

Figure 11. Isoenergy (P – ϕ') maps for various 3′-mononucleotides containing adenine as a representative purine base: (a) α-3′-dAMP, (b) α-3′-AMP, (c) β-3′-dAMP, and (d) β-3′-AMP. See caption to Figure 5 for other details.

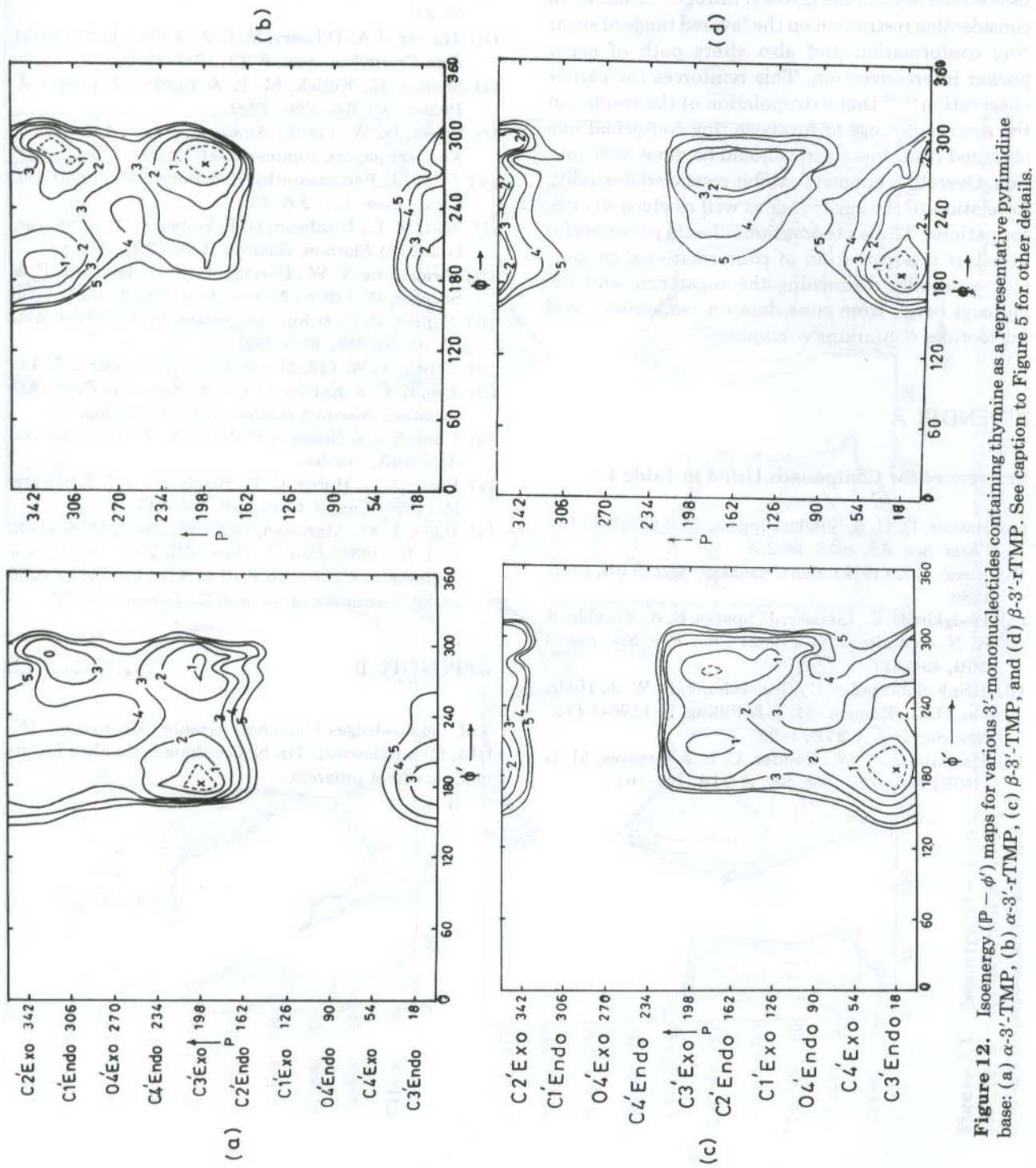

Figure 12. Isoenergy ($\mathbb{P} - \phi'$) maps for various 3'-mononucleotides containing thymine as a representative pyrimidine base: (a) α-3'-TMP, (b) α-3'-rTMP, (c) β-3'-TMP, and (d) β-3'-rTMP. See caption to Figure 5 for other details.

though it is implied that sugar pucker undergoes interconversion. It is also found that inclusion of base atoms beyond the glycosyl nitrogen brings forth considerable restriction on the favored range of sugar ring conformation and also alters path of sugar pucker interconversion. This reinforces the earlier observation[33–35] that extrapolation of the results on the preferred range of furanose ring conformations obtained from free sugars should be done with caution. Overall, α-anomers exhibit restricted flexibility in relation to the sugar ring as well as glycosyl conformations. These observations should prove useful in better interpretation of conformational properties, especially concerning the sugar ring and the glycosyl bond, from nmr data on nucleosides and nucleotides containing α-anomers.

APPENDIX A

References for Compounds Listed in Table I

(a) Rohrer, D. C. & Sundaralingam, M. (1970) *J. Am. Chem. Soc.* **92,** 4956–4962.

(b) Ruzic, J.-Z. (1979) *Acta Crystallogr. Sect. B* **35,** 1277–1280.

(c) Hodgkin, D. C., Lindsey, J., Sparks, R. A., Trueblood, K. N. & White, J. G. (1962) *Proc. Roy. Soc. Ser. A* **266,** 494–517.

(d) Brink-Shoemaker, C., Cruickshank, D. W. J., Hodgkin, D. C., Kamper, M. J. & Pilling, D. (1964) *Proc. Roy. Soc. Ser. A* **278,** 1–26.

(e) Hawkinson, S. W., Coulter, C. L. & Greaves, M. L. (1970) *Proc. Roy. Soc. Ser. A* **318,** 143–167.

(f) Savage, H. F. J., Lindley, P. F., Finney, J. L. & Timmins, P. A. (1987) *Acta Cryst. B* **43,** 280–295.

(g) Lenhert, P. G. (1968) *Proc. Roy. Soc. Ser. A* **303,** 45–84.

(h) Hamor, J. A., O'Leary, M. K. & Walker, R. T. (1977) *Acta Crystallogr. Sect. B* **33,** 1218–1223.

(i) Shefter, E., Kotick, M. P. & Bardos, J. (1967) *J. Pharm. Sci.* **56,** 1293–1299.

(j) Frank, G. W. (1968) American Cryst. Association, Abstract papers, summer meeting, 99.

(k) Vitali, J., Parthasarathy, R. & Bobek, M. (1979) *Am. Cryst. Assoc. Ser. 2* **6,** 68.

(l) Post, M. L., Birnbaun, G. I., Huber, C. P. & Shugar, D. (1977) *Biochim. Biophys. Acta* **479,** 133–142.

(m) Armstrong, V. W., Dattagupta, J. K., Eckstein, F. & Saenger, W. (1976) *Nucleic Acids Res.* **3,** 1791–1810.

(n) Rohrer, D. C. & Sundaralingam, M. (1970) *J. Am. Chem. Soc.* **92,** 4950–4955.

(o) Tench, A. W. (1980) *Am. Cryst. Assoc. Ser. 2* **7,** 14.

(p) Lee, K. C. & Kartha, G. (1974) American Cryst. Association, Abstract papers, summer meeting, 273.

(q) Cline, S. J. & Hodgson, D. J. (1979) *Biochim. Biophys. Acta* **563,** 540–544.

(r) Post, M. L., Huber, C. P., Birnbaun, G. I. & Shugar, D. (1981) *Can. J. Chem.* **59,** 238–245.

(s) Piper, I. M., MacLean, D. B., Faggiani, R. & Lock, C. J. L. (1985) *Can. J. Chem.* **63,** 2915–2921. X coordinate of C1′ has to read as 9236 instead of 0236 and Z coordinate of O4′ as 6323 instead of 4323.

APPENDIX B

YSL acknowledges University Grants Commission, INDIA, for a fellowship. Dr. N. Gautham is thanked for the molecular plot program.

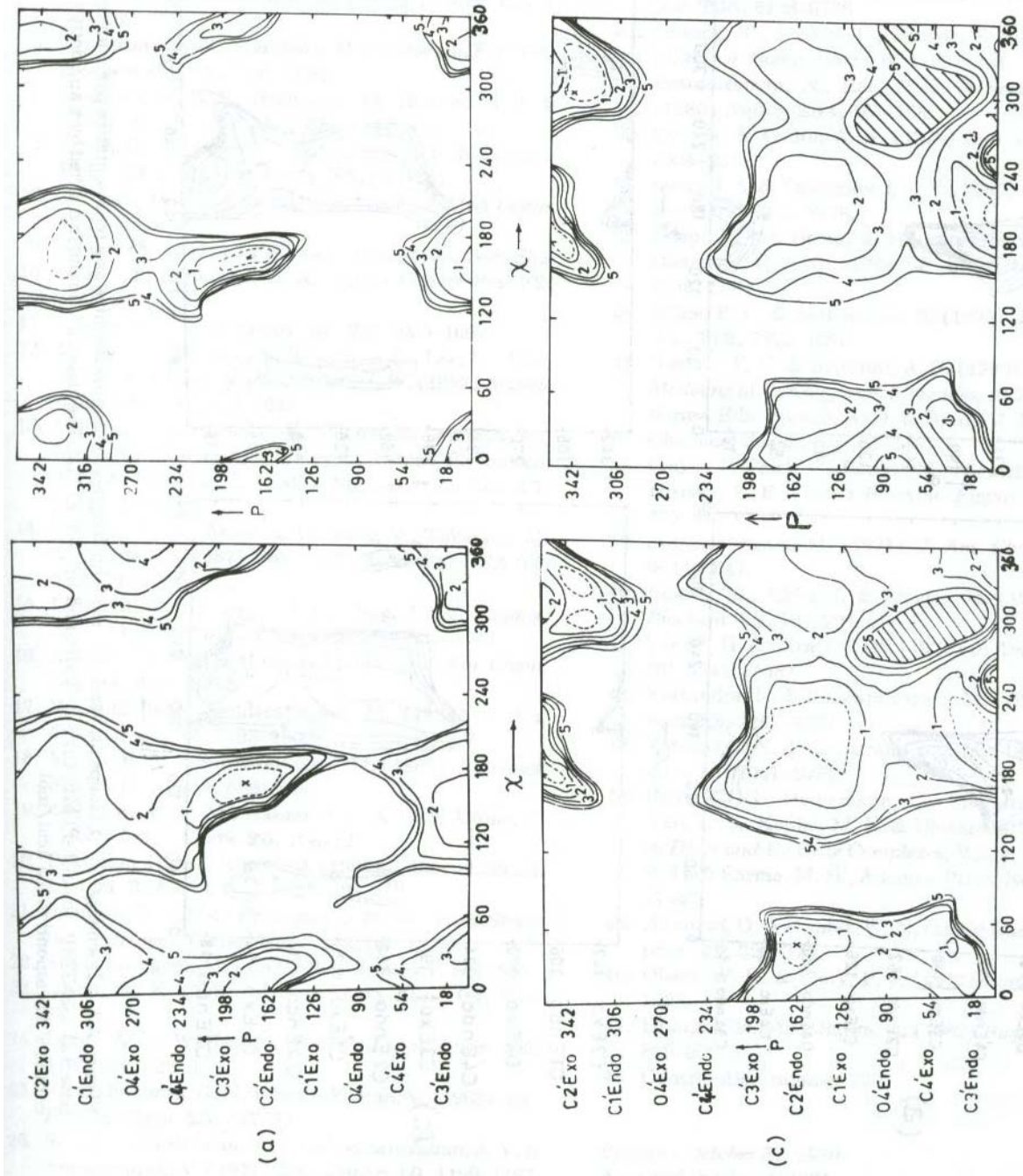

Figure A1. Isoenergy (P − χ) maps for various 3′-mononucleotides containing adenine as a representative purine base: (a) α-3′-dAMP, (b) α-3′-AMP, (c) β-3′-dAMP and (d) β-3′-AMP. The global minimum is marked by x and dotted contours correspond to 0.5 kcal/mol.

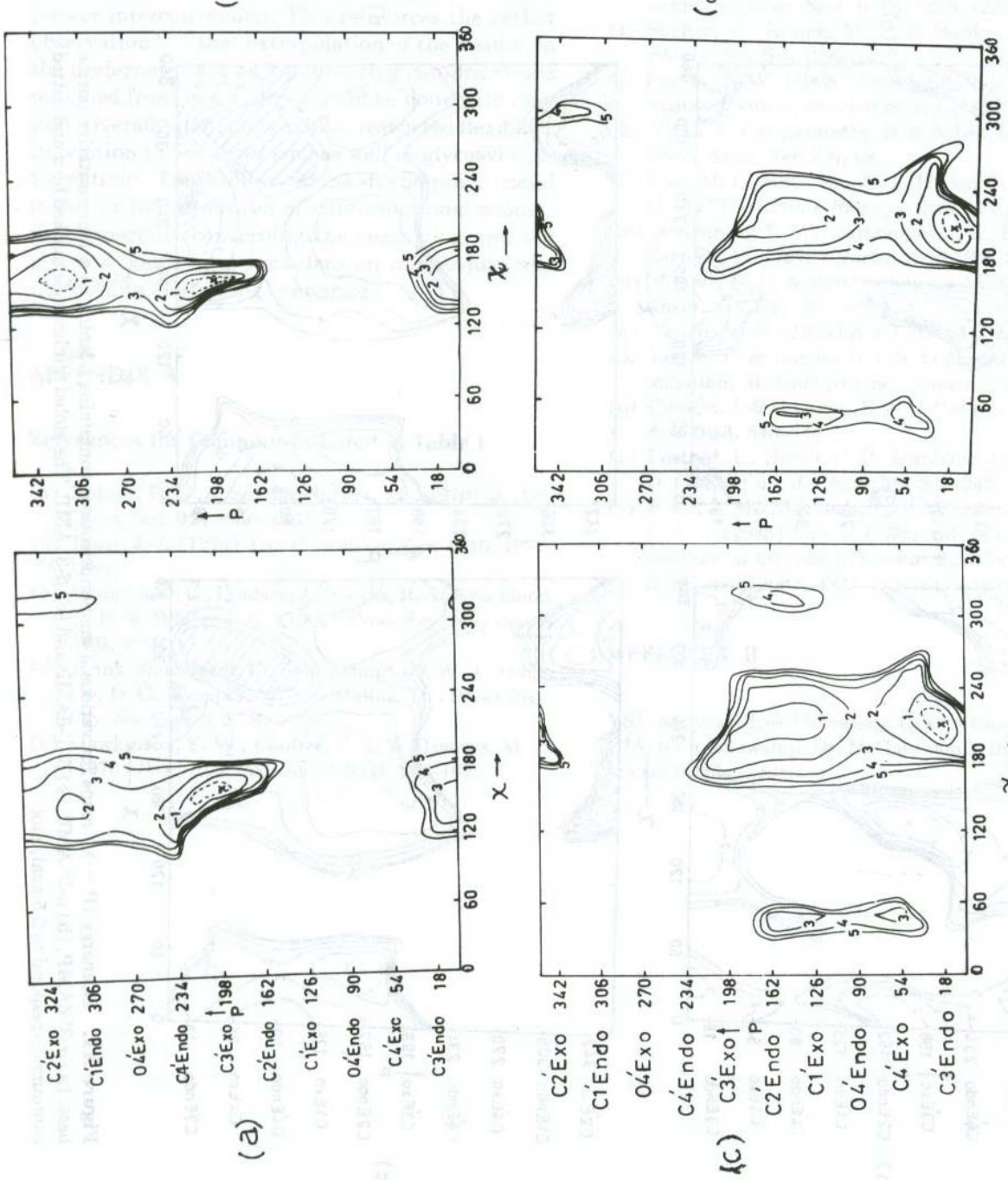

Figure A2. Isoenergy (P − χ) maps for various 3′-mononucleotides containing thymine as a representative pyrimidine base: (a) α-3′-TMP, (b) α-3′-rTMP, (c) β-3′-TMP, and (d) β-3′-rTMP. The global minimum is marked by x and dotted contours correspond to 0.5 kcal/mol.

REFERENCES

1. Suzuki, K., Nakano, H. & Suzuki, S. (1967) *J. Biol. Chem.* **242,** 3319–3325.
2. Bonnett, R. (1963) *Chem. Rev.* **63,** 573–605.
3. Holy, A. (1973) *Coll. Czech. Chem. Commun.* **38,** 100–114.
4. Kulikowski, T. & Shugar, D. (1974) *J. Med. Chem.* **17,** 269–273.
5. Armstrong, V. W., Sternbach, H. & Eckstein, F. (1976) *Biochemistry* **15,** 2086–2091.
6. Christensen, L. F., Broom, A. D., Robins, M. J. & Bloch, A. (1972) *J. Med. Chem.* **15,** 735–739.
7. Smith, C. W., Sidwell, R. W., Robins, R. K. & Tolman, R. L. (1972) *J. Med. Chem.* **15,** 883–887.
8. Milne, G. H. & Townsend, L. B. (1974) *J. Med. Chem.* **17,** 263–268.
9. Shugar, D. (1974) *FEBS Lett.* **40**(suppl.), S48–S52.
10. Nakai, Y. & Lepage, G. A. (1972) *Cancer Res.* **32,** 2445–2451.
11. Sequin, U. (1973) *Experientia* **29,** 1059–1062.
12. Morvan, F., Rayner, B., Imbach, J.-L., Lee, M., Hartley, J. A., Chang, D.-K. & Lown, J. W. (1987) *Nucleic Acids Res.* **15,** 7027–7043.
13. Gagnor, C., Bertrand, J.-R., Thenet, S., Lemaitre, M., Morvan, F., Rayner, B., Malvy, C., Lebleu, B., Imbach, J.-L. & Paoletti, C. (1987) *Nucleic Acids Res.* **15,** 10419–10436.
14. Thuong, N. T., Asseline, U., Roig, V., Takasugi, M. & Helene, C. (1987) *Proc. Natl. Acad. Sci. USA* **84,** 5129–5133.
15. Lancelot, G., Guesnot, J.-L., Roig, V. & Thuong, N. T. (1987) *Nucleic Acids Res.* **15,** 7531–7547.
16. Altona, C. & Sundaralingam, M. (1972) *J. Am. Chem. Soc.* **94,** 8205–8212.
17. Westhof, E. & Sundaralingam, M. (1980) *J. Am. Chem. Soc.* **102,** 1493–1500.
18. Meritt, E. A. & Sundaralingam, M. (1985) *J. Biomol. Struct. Dynam.* **3,** 559–578.
19. de Leeuw, H. P. M., Haasnoot, C. A. G. & Altona, C. (1980) *Isr. J. Chem.* **20,** 108–126.
20. Pearlman, D. A. & Kim, S. H. (1985) *J. Biomol. Struct. Dynam.* **3,** 85–98.
21. Saenger, W. (1984) *Principles of Nucleic Acid Structure,* Springer-Verlag, New York, pp. 51–55.
22. Sundaralingam, M. (1969) *Biopolymers* **7,** 821–827.
23. Olson, W. K. (1982) *J. Am. Chem. Soc.* **104,** 278–286.
24. Levitt, M. & Warshel, A. (1978) *J. Am. Chem. Soc.* **100,** 2607–2613.
25. Ramachandran, G. N. & Sasisekharan, V. (1968) *Adv. Protein Chem.* **23,** 347–367.
26. Renugopalakrishnan, V., Lakshminarayanan, A. V. & Sasisekharan, V. (1971) *Biopolymers* **10,** 1159–1167.
27. Saran, A., Pullman, B. & Perahia, D. (1973) *Theor. Chim. Acta* **30,** 31–44.
28. Rao, N. S. & Sasisekharan, V. (1981) *Ind. J. Biochem. Biophys.* **18,** 303–310.
29. Pearlman, D. A. & Kim, S. H. (1985) *J. Biomol. Struct. Dynam.* **3,** 99–125.
30. Harvey, S. C. & Prabhakaran, M. (1986) *J. Am. Chem. Soc.* **108,** 6128–6136.
31. Schlick, T., Peskin, C., Broyde, S. & Overton, M. (1987) *J. Comp. Chem.* **8,** 1199–1224.
32. Pattabiraman, N., Rao, N. S. & Sasisekharan, V. (1980) *Nature* **284,** 187–188.
33. Cyr, N. & Perlin, A. S. (1979) *Can. J. Chem.* **57,** 2504–2511.
34. Gerlt, J. A. & Youngblood, A. V. (1980) *J. Am. Chem. Soc.* **102,** 7433–7438.
35. Raap, J., van Boom, J. H., van Lieshout, H. C. & Haasnoot, C. A. G. (1988) *J. Am. Chem. Soc.* **110,** 2736–2743.
36. Kline, P. C. & Serianni, A. S. (1990) *J. Am. Chem. Soc.* **112,** 7373–7381.
37. Garrett, E. C. & Serianni, A. S. (1989) in *Computer Modeling of Carbohydrate Molecules,* ACS Symposium Series, Eds. French, A. D. & Brady, J. N., American Chemical Society, pp. 91–119.
38. Cadet, J., Taieb, C., Remin, M., Niemczura, W. P. & Hruska, F. E. (1980) *Biochim. Biophys. Acta* **608,** 435–445.
39. Sundaralingam, M. (1971) *J. Am. Chem. Soc.* **93,** 6644–6647.
40. Remin, M., Ekiel, I. & Shugar, D. (1975) *Eur. J. Biochem.* **53,** 197–206.
41. Lee, C.-H. & Sarma, R. H. (1976) *J. Am. Chem. Soc.* **98,** 3541–3548.
42. Yathindra, N. & Sundaralingam, M. (1973) *Biopolymers* **12,** 2261–2277.
43. Yathindra, N. & Sundaralingam, M. (1974) *Biopolymers* **13,** 2061–2076.
44. Prive, G. G., Heinemann, U., Chandrasegaran, S., Kan, L.-S., Kopka, M. L. & Dickerson, R. E. (1988) in *DNA and Its Drug Complexes,* Vol. 2, Eds., Sarma, R. H. & Sarma, M. H., Adenine Press, New York, pp. 27–47.
45. Kennard, O. & Hunter, W. N. (1989) *Quart. Rev. Biophys.* **22,** 327–379.
46. Olson, W. K. & Flory, P. J. (1972) *Biopolymers* **11,** 1–28.
47. Dhingra, M. M. & Saran, A. (1982) *Biopolymers* **21,** 859–872.
48. Contribution number 780.

Received October 31, 1990
Accepted October 4, 1991